RP Current Trends in Engineering and Technology
Vol. 2, No. 1 (January – March 2023) pp. 8–12
e-ISSN: 2583-5491

RESEARCH PLATEAU PUBLISHERS

Cite this article: Surila, Synthesis and characterization of nickel oxide nanoparticles by sol-gel technique, *RP Cur. Tr. Eng. Tech.* **2** (2023) 8–12.

Original Research Article

Synthesis and characterization of nickel oxide nanoparticles by sol-gel technique

Surila
Department of Chemistry, Government P.G. Nehru College, Jhajjar – 124103, Haryana, India
*Corresponding author, E-mail: surilachanderbhan@gmail.com

ARTICLE HISTORY
Received: 5 Oct. 2022
Revised: 30 Dec. 2022
Accepted: 10 Jan. 2023
Published online: 11 Jan. 2023

KEYWORDS
Nickel oxide nanoparticles; XRD; SEM; TGA-DTA.

ABSTRACT
By using the Sol-Gel process, NiO nanoparticles were created, and they were then annealed at various temperatures. The powders were examined using TGA, scanning electron microscopy, and x-ray diffraction. By using x-ray diffraction to characterise the structure of the films, it was confirmed that they were polycrystalline and had a cubic structure. The results of the SEM study of the films allowed researchers to draw the conclusion that the manufactured films are uniform, rough, include big crystals, and exhibit particle agglomeration. The sample's thermal stability was investigated using TGA analysis, which revealed that NiO nanoparticles formed between 130 and 720°C.

1. Introduction

In comparison to their bulk counterparts, metal oxide nanomaterials exhibit much greater chemical, mechanical, electrical, thermal, magnetic, catalytic, and optical capabilities, and they have attracted a wide range of applications [1, 2]. Because of their high surface area to volume ratio, quick diffusivities, peculiar adsorptive qualities, and surface imperfections, nanosized crystalline metal oxides have attracted more attention in recent years than larger crystalline metal oxides [3]. Oxygen belongs to Block P, Period 2, whereas nickel belongs to Block D, Period 4.

The application of nickel oxide in many different fields, including electrochromic films [4-6], fuel cell electrodes [7] and gas sensors [8–10], battery cathodes [11–15], pn heterojunctions [16–18], magnetic materials [19–20], photovoltaic devices [21–22], electrochemical supercapacitors [23–24], smart windows [23], and dye-sensitized photocathodes [24], has attracted a lot of attention.

For the majority of these applications, tiny particles with a narrow size distribution are necessary. NiO nanoparticles are anticipated to have much more enhanced properties and even more alluring applications than bulk-sized NiO particles thanks to the volume effect, quantum size effect, and surface effect. Depending on the particle size, shape, and synthesis method, NiO nanostructures, for instance, can exhibit super-paramagnetic, super-anti-ferromagnetic, or ferromagnetic order magnetic properties, but bulk NiO is an anti-ferromagnetic insulator with a Neel temperature (T_N) of 523 K.

The solution phase chemistry approach is used to prepare nickel, and in theory this should offer a variety of straightforward ways to regulate the desired crystalline phase, particle size, and morphology. The development of nickel oxide nanoparticle production techniques that allow for precise control over the final products' crystal structure and particle size is crucial.

The Sol Gel process was used to create the Nickel Oxide nanoparticles, which were then annealed at two distinct temperatures, 500°C and 700°C. Using the use of XRD, SEM, and TGA-DTA, the impact of annealing on produced Nickel Oxide nanoparticles has been thoroughly examined and described.

2. Materials and methods

One of the easiest, safest for the environment, and least expensive methods for making pure transition metal oxides at low temperatures with a high specific surface area is sol gel preparation. Also, this approach may be advantageous because to its straightforward operation, high product yield, minimal energy usage, and lack of specialised equipment.

The four key steps in the Sol-Gel process for making materials are: (i) generating the solution (sol), (ii) shaping and gelling it, (iii) drying, and (iv) conglomeration. Figure 1 shows a schematic illustration of the Sol-Gel process.

Step 1: In 25ml of ethanol and isopropyl alcohol, dissolve 0.1M of nickel acetate.

Step 2: Stirring the precursor solution until a clear solution forms.

Step 3: To achieve a pH of 9, sodium oxide was then gradually added.

Step 4: The sol is created and the magnetic stirrer's temperature is raised above 70°C.

Step 5: The green colour gel was generated after two hours, and it was washed with ethanol three to five times to get rid of byproducts and unreacted substances.

Step 6: The Gel is then heated to 100°C for 24 hours in a hot air oven.

Step 7: A muffle furnace is used to anneal the dry powder at various annealing temperatures (500°C and 700°C).

Step 8: During the annealing procedure, the green NiO nanoparticles turn black in colour.

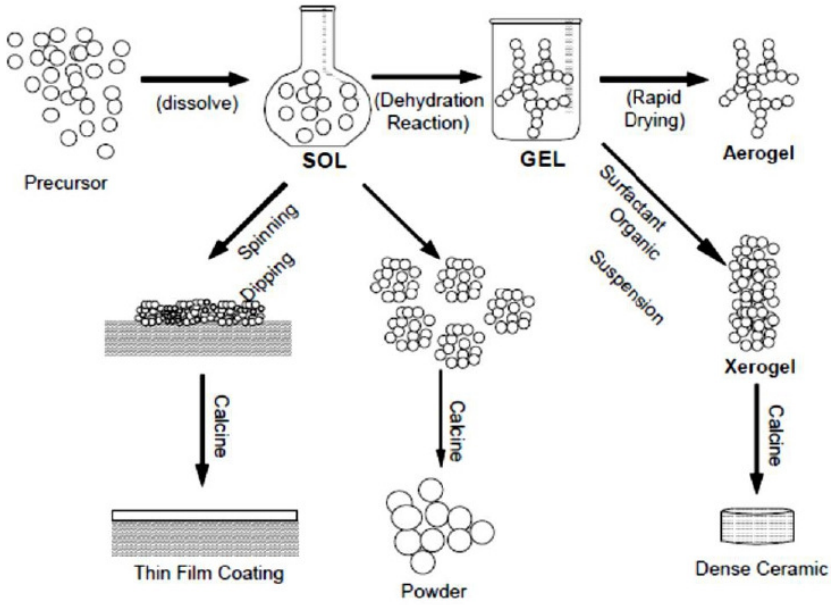

Figure 1: Sol-gel technique for the production of nanomaterials is shown schematically. NiO nanoparticles are created using the Sol-Gel technique.

(a) **(b)**

Figure 2: (a) Before annealing NiO Nanoparticles; **(b):** After annealing NiO Nanoparticles.

3. Results and discussion

3.1 Structural analysis

Figure 3 displays the X-Ray Diffraction pattern of Nickel Oxide nanoparticles, which was obtained with λ = 1.54Å and a theta range of 20-90 degrees. The sample has good crystallinity as evidenced by the predominate peaks, which are located in the (200), (111), and (220) planes. The technique yields NiO nanoparticles with an average grain size of 14.08 nm. The cubic structure of the nickel oxide sample, with a = 4.17Å, is consistent with JCPDS file 47-1049 [25]. The XRD pattern of NiO nanoparticles annealed at 700°C is shown in Figure 4. The main peaks are located in the plane at high intensities (200), (111), and (220). The particle's average grain size is determined to be 15.86 nm. The NiO nanoparticles that were annealed at 700°C have somewhat bigger grains than those that were annealed at 500°C. This indicates that grain size grows larger as temperature rises. This behaviour was anticipated since heating promotes particle diffusion and agglomeration [26–28].

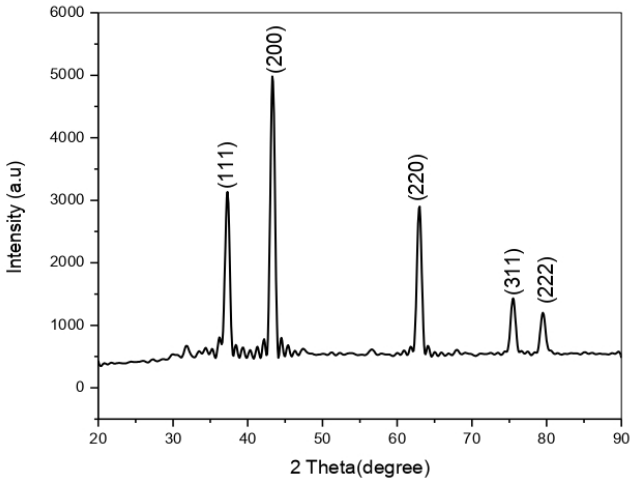

Figure 3: XRD Pattern of NiO nanoparticles annealed at 500°C.

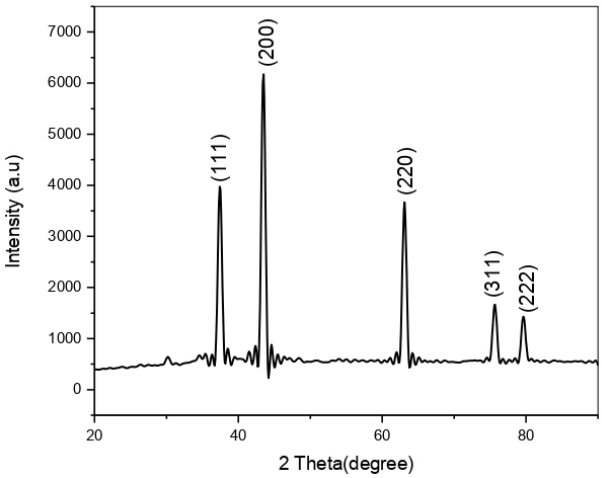

Figure 4: XRD Pattern of NiO nanoparticles annealed at 700°C.

Because the crystallite size will be huge at higher temperatures, the diffraction peaks will become more strong. The thermally enhanced crystallite formation is responsible for this [29]. The XRD characteristics of NiO nanoparticles annealed at two different temperatures are provided in Table 1. The cubic structure of the NiO nanoparticles with lattice parameters of $a = b = c = 4.17$Å is evident from the table.

Table 1: XRD parameters of NiO nanoparticles.

Sample	hkl plane	2 Theta (degree)	Theta (degree)	Grain size (nm)	Lattice constant ($a = b = c$)
NiO nanoparticles annealed at 500°C	111	37.24	18.82	13.22	4.177
	200	43.29	21.64	13.88	4.176
	220	62.90	31.45	15.15	4.175
	311	75.43	37.71	15.38	4.173
	222	79.42	39.71	15.99	4.176
NiO nanoparticles annealed at 700°C	111	37.40	18.70	14.92	4.160
	200	43.44	21.72	15.59	4.162
	220	63.03	31.51	17.06	4.167
	311	75.58	37.79	17.96	4.169
	222	79.57	39.78	19.41	4.169

3.2 Surface morphological analysis

SEM was used to examine the surface morphological characteristics of produced nanoparticles. Figure 5 displays the SEM picture of NiO nanoparticles at 10,000, 20,000, and 55,000 times their original size. On the SEM image are the instrument characteristics, accelerating voltage, spot size, magnification, and working distances. Some particles appear to be spherical in shape. We can see that the particles are essentially a cluster of nanoparticles and are heavily agglomerated. Because NiO nanoparticles have a propensity to aggregate due to their high surface energy and high surface tension of the ultrafine nanoparticles, the observation of some bigger nanoparticles may be explained by this [30].

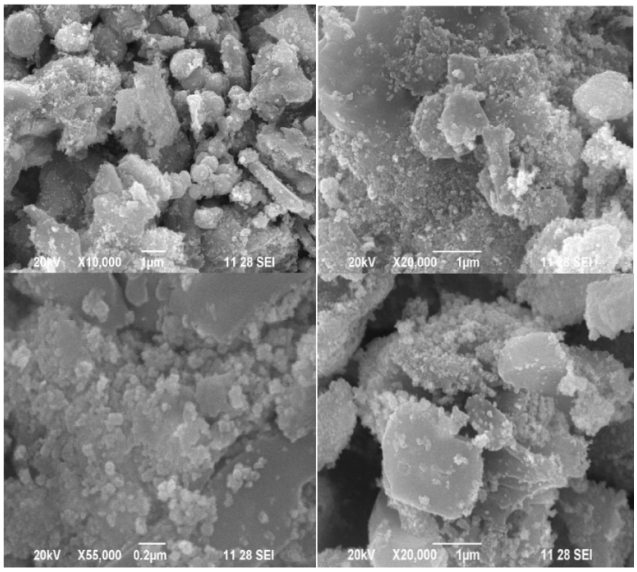

Figure 5: SEM images of NiO nanoparticles annealed at 500°C.

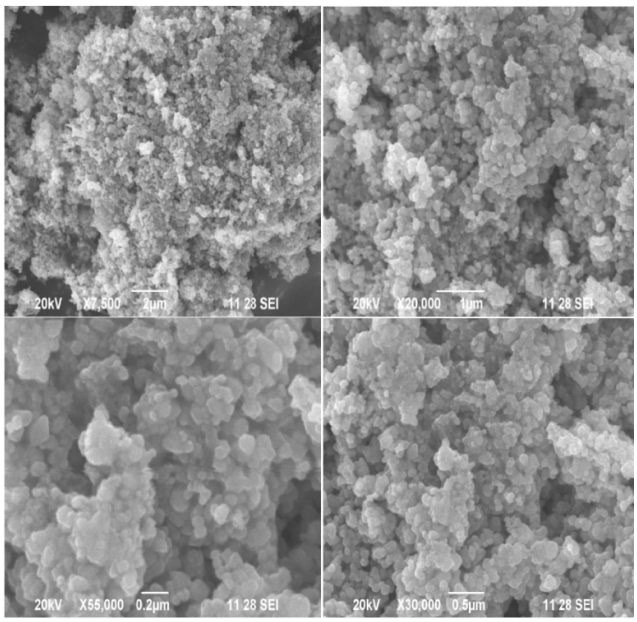

Figure 6: SEM images of NiO nanoparticles annealed at 700°C.

Figure 6 displays SEM micrographs that were magnified between 7,500 and 30,000 times and annealed at 700°C. The particles include some sphere-shaped ones. Agglomerated particles are made up of evenly spaced out particles that are joined together. The size of the aggregates grows as the annealing temperature rises from 500 to 700°C; this agglomeration causes the crystallite size of the particles to grow [31].

3.3 Thermal analysis

Many substances are unstable and break down into different substances when heated. Thermo gravimetric analysis is used to characterise the prepared sample in order to determine its thermal stability. The TGA curve of synthetic NiO that was annealed at 700°C and varied in temperature from 40 to 730°C is shown in Figure 7(a). There are two stages to the weight loss: (i) dehydration-related weight loss of 0.5% between 80 and 90 degrees [32], (ii) 100–120°C, with a weight loss of 0.3% as a result of water evaporation.

Around 89°C, a clear endothermic peak can be seen in the DTA curve. This could be explained by the precursor's thermal dehydration and the evaporation of physically adsorbate contaminants. The NiO crystal phase is anticipated to emerge when the hydroxyl group from $Ni(OH)_2$ is eliminated (Figure 7(b)).

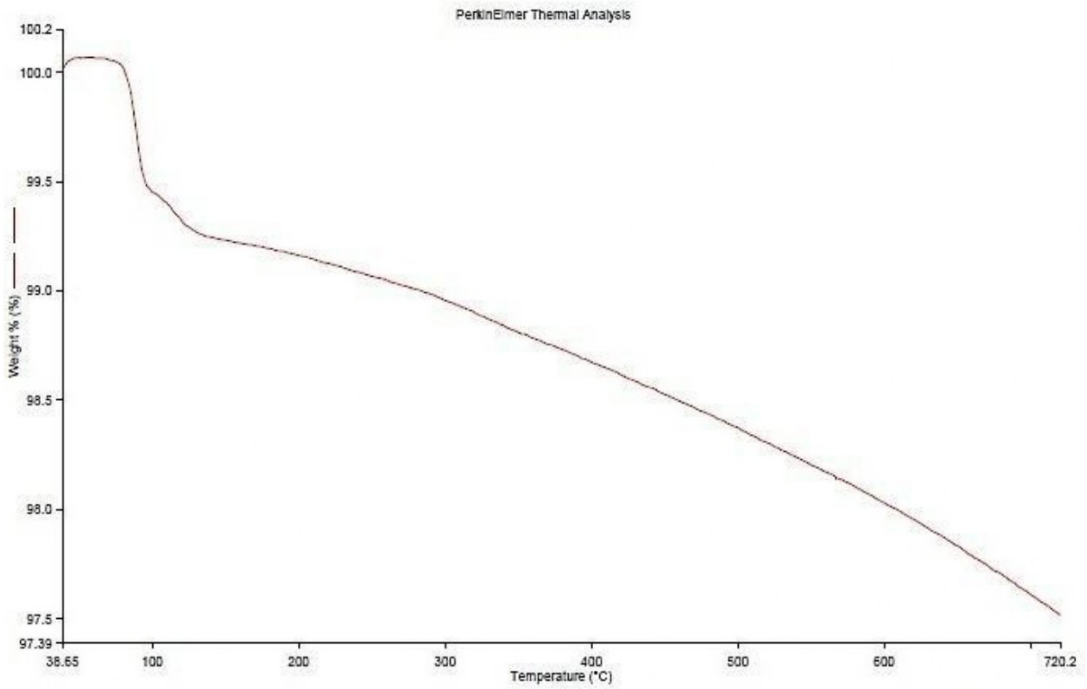

Figure 7(a): TGA curve of NiO nanoparticles annealed at 700°C.

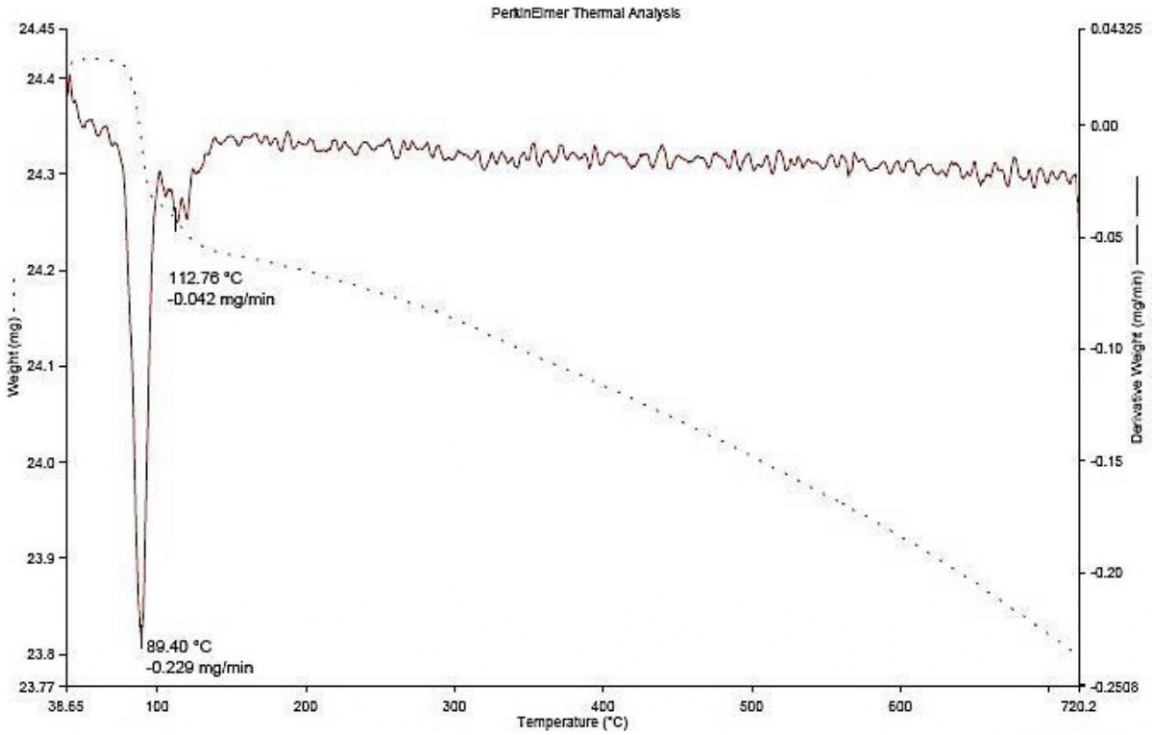

Figure 7(b): DTA curve of NiO nanoparticles annealed at 700°C.

4. Conclusions

The Sol Gel process was used to create the Nickel Oxide nanoparticles, which were then annealed at two distinct temperatures, 500°C and 700°C. The grain size of the samples grows with increasing annealing temperature, according to XRD measurements. According to SEM findings, the particles are essentially a cluster of nanoparticles and are heavily agglomerated. The sample's thermal stability was investigated using TGA analysis, which revealed that NiO nanoparticles formed between 130 and 720°C. Lithium ion microbatteries and ceramic structures can both be made using the prepared nickel oxide.

Acknowledgements

The author would like to thank Prof. Ashish Agarwal, Department of Physics, Guru Jambheshwar University of Science & Technology, Hisar – 125001 (Haryana) India for providing the necessary facilities to synthesize the materials

and their characterization in their Materials Science Laboratory.

References

[1] Q. Li, L.S. Wang, B.Y. Hu, C. Yang, L. Zhou, L. Zhang, Preparation and characterization of nanoparticles through calcination of malate gel, *Mater. Lett.* **61** (2007) 1615-1618.

[2] X. Xin, Z. Lü, B. Zhou, Effect of synthesis conditions on the performance of weakly agglomerated nanocrystalline, *J. Alloys Comp.* **42** (2007) 251-255.

[3] Y. Wu, Y. He, T. Wu, T. Chen, W. Weng, H. Wan, Influence of some parameters on the synthesis of nanosized material by modified sol-gel method, *Mater. Lett.* **61** (2007) 3174-3178.

[4] K.K. Purushothaman, G. Muralidharan, Nanostructured NiO based all solid state electrochroic device, *J. SolGel Sci. Tech.* **46** (2008) 190-194.

[5] J.L. Garcia-Miquel, Q. Zhang, S.J. Allen, A. Rougier, A. Blyr, H.O. Davies, Nickel oxide Sol-Gel films from Nickel diacetate for electrochromic applications, *Thin Solid Films* **424** (2003) 165-170.

[6] W.Y. Li, L.N. Xu, J. Chen, CO_3O_4 nanomaterials in Lithium-ion batteries and Gas sensors, *Adv. Funct. Mater.* **15** (2005) 851-857.

[7] F. Li, H.Y. Chen, C.M. Wang, K.S. Hu, A novel modified NiO cathode for molten carbonate fuel cells, *J. Electroanal. Chem.* **531** (2002) 53-60.

[8] Hotovy, J. Huran, L. Spiess, S. Hascik, V. Rehacek: Sens, Preparation of Nio thin films for Gas sensor applications, *Actuators B Chem.* **57** (1999) 147-152.

[9] E.L. Miller, R.E. Rocheleau, Electrochemical behaviour of relatively sputtered iron-doped nickel oxide, *J. Electrochem. Soc.* **144** (1997) 3072-3077.

[10] H.X. Yang, Q.F. Dong, X.H. Hu, X.P. Ai, S.X. Li, Preparation and characterization of $LiNiO_2$ synthesized from $Ni(OH)_2$ and LiOH centre dot H_2O, *J. Power Sources* **79** (1999) 256-261.

[11] F.B. Zhang, Y.K. Zhou, H.L. Li., Nanocrystalline NiO as an electrode material for electrochemical capacitor, *Mater. Chem. Phys.* **83** (2004) 260-264.

[12] Hotovy, J. Huran, L. Spiess, Preparation and characterization of NiO thin films for gas sensor applications, *Vacuum* **58** (2000) 300-307.

[13] X.H. Huang, J.P. Tu, B. Zhang, C.Q. Zhang, Y. Li, Y.F. Yuan, H.M. Wu, Electrochemical properties of NiO–Ni nanocomposite as anode material for lithium ion batteries, *J. Power Sources* **161** (2006) 541-544.

[14] D. Leevin, J.Y. Ying, Oxidative dehydrogenation of propane by non-stoichiometric nickel molybdates, *Stud. Surf. Sci. Catal.* **110** (1997) 367-373.

[15] M. Yoshio, Y. Todorov, K. Yamato, H. Noguchi, J. Itoh, M. Okada, T. Mouri, Preparation of LIYMNXNI XO_2 as a cathode for lithium ion batteries, *J. Power Sources* **74** (1998) 46-53.

[16] Chrissanthopoulos, S. Baskoutas, N. Bouropoulos, V. Dracopoulos, P. Poulopoulos, S.N. Yannopoulos, Synthesis and Characterization of ZnO/NiO p-n heterojunctions: ZnO nanorods grown on NiO thin film by thermal evaporation, *Photon Nanostructures* **9** (2011) 132-139.

[17] L.G. Teoh, K.D. Li, Synthesis and characterization of NiO nanoparticles by solgel method, *Mater. Trans*. **53** (2012) 2135 2140.

[18] M. Ghosh, K. Biswas, A. Sundaresan, C.N.R. Rao, MnO and NiO nanoparticles: Synthesis and magnetic properties, *J. Mater. Chem.* **16** (2006) 106-111.

[19] L. Del Bianco, F. Boscherini, M. Tamisari, F. Spizzo, M. Vittori Antisari, E. Piscopiello, Exchange bias and interface structure in the Ni/NiO nanogranular system, *J. Phys. D: Appl. Phys.* **41** (2008) 134-008.

[20] T. Ahmad, K.V. Ramanujachary, S.E. Lofland, A.K. Ganguli, Magnetic and electrochemical properties of nickel oxide nanoparticles obtained by reverse-micellar route, *Solid State Sci.* **8** (2006) 425-430.

[21] M. Borgstrom, E. Blart, G. Boschloo, E. Mukhtar, A. Hagfeldt, L. Hammarstrom, Sensitized hole injection of phosphorousporphyrin into NiO: towards new photovoltaic devices, *J. Phys. Chem. B* **109** (2005) 22928-22934.

[22] T. Nathan, A. Aziz, A.F. Noor, S.R.S. Prabaharan, Nanaostructured NiO for electrochemical capacitors: Synthesis and electrochemical properties, *J. Solid State Electrochem.* **12** (2008) 1003-1009.

[23] C.G. Granqvist, *Handbook of Inorganic Electrochromic Materials*, Elsevier, Amsterdam (1995).

[24] J. He, H. Lindström, A. Hagfeldt, S.E. Lindquist, *J. Phys. Chem. B* **103** (1999) 8940-8943.

[25] R. Martin, G. Mc Carthy, North Dakota State University, Fargo, ND,USA, ICDD, Grant-in-aid (1991).

[26] N.M. Ghoneim, S. Hanafi, S.A. Abo El-enein, Characteristics and effect of thermal- treatment on surface texture of ultrafine zirconia powders, *J. Mater Sci*. **22** (1987) 791-797.

[27] A. Cabot et al., Synthesis of tin oxide nanostructures with controlled particle size using mesoporous frameworks, *Electrochem. Solid-State Lett*. **7** (2004) G93-G97.

[28] J. Lu, Z.Z. Fang, Synthesis and characterization of nanoscaled cerium (IV) oxide via a solid state mechanochemical method, *J. Am. Ceramic. Soc.* **89** (2006) 842-847.

[29] P.A. Sheena et al., Effect of calcination temperature on the structural and optical properties of nickel oxide nanoparticles, *Nanosystems: Physics, Chemistry and Mathematics* **5** (2014) 441-449.

[30] M.N. Rifaya, T. Theivasanthi, M. Alagar, Chemical capping synthesis of nickel oxide nanoparticles and their characterizations studies, *Nanosci. Nanotech.* **2** (2012) 134-138.

[31] Abd El-Aziz A.Said, Mohamed M.Abd El-Wahab, Soliman A. Soliman, M.N. Goda, Synthesis and characterization of nano CuO-NiO mixed oxides, *Nanosci. Nanoeng.* **2** (2014) 17-28.

[32] Umbreen Ashraf, Bushra Khan, Synthesis and characterization of nickel oxide nanopowder by sol-gel method, *Int. J. Sci. Res.* **4** (2015) 2405-2408.